BFUT P26

Singularity: Why and How Physical Substrate Dynamics Make Infinite Density Impossible

Finite-Core Compact Object Structure, the Rotational Sustenance Principle, and Nine Popular Myths Refuted

Vijay Shankar Sharma

Independent Researcher, Gurugram, National Capital Region, India

vss@vijayshankarsharma.com | ORCID: 0009-0001-9622-6121

DOI: 10.5281/zenodo.20557070

 | No external funding | No conflicts of interest

Abstract

General Relativity (GR) successfully models gravitational curvature and geodesic motion but permits singularities because curvature is treated geometrically without a physically compressible carrier medium possessing persistence, redistribution, entrainment, saturation, and coherence dynamics. This paper proposes that when gravitational deformation is treated as physically real and dynamically propagated through the Spaticle field [4] substrate, five stabilising mechanisms emerge naturally: outward rotational entrainment redistribution, finite propagation effects, nested-domain reinforcement [6], vortex-core stabilisation, substrate restoring pressure, and coherence-threshold saturation. Together these mechanisms prevent unlimited local density divergence and replace singular collapse with finite organised compression structures whose maximum density ρ_max_finite is bounded by the same substrate parameters that govern galaxy rotation curves and gravitational-wave carrier dynamics. The paper derives the maximum compression density bound from the full extended free-energy functional of the Spaticle field [4], where all stabilising terms originate from one substrate density $\rho_s = 5.9 \times 10^{-27}$ kg/m³ and the proton charge radius r_p with no additional free parameters. The Rotational Sustenance Principle is introduced: no vortical compression core of any origin can persist without a continuous supply of surrounding rotating mass. A quantitative seed dissipation timescale τ_dissip = R_d/c is derived - approximately 59 minutes for a 10 M☉ isolated seed core - establishing that Pathway 2 (stellar collapse) and Pathway 3 (explosive release) seed cores are genuinely transient without rotational reinforcement [6], while Pathway 1 (large-scale rotational aggregation) cores are inherently self-sustaining. Quantitative analysis of DDR enhancement fractions across ten validated SPARC galaxies provides direct observational evidence for rotational entrainment saturation. Nine popular myths about

singularities are systematically addressed. Four falsifiable predictions are presented. [19]

Keywords: singularity, Spaticle field, free-energy functional, finite compression core, rotational entrainment, Rotational Sustenance Principle, seed dissipation timescale, information paradox, Penrose-Hawking theorems, BFUT [17, 18]

---

1. Introduction

Singularities arise in standard GR because inward collapse amplification possesses no intrinsic physical redistribution mechanism. Curvature modifies trajectories mathematically, but the curvature field itself is not treated as a physically organised medium capable of storing deformation energy, redistributing organised stress outward, propagating entrainment into surrounding regions, resisting compression through restoring pressure, exhibiting coherence thresholds, or dynamically relaxing after a disturbance. In standard GR, curvature exists geometrically. In the present framework, curvature and deformation correspond to organised compression states within the Spaticle field [4] - a real continuous elastic substrate filling all space with equilibrium density $\rho_s = 5.9 \times 10^{-27}$ kg/m³, independently constrained across seven physical sectors spanning forty orders of magnitude from W and Z boson masses at the femtometre scale to galaxy rotation curves at the megaparsec scale [13].

The central thesis is that once curvature is treated as a physically real organised deformation state embedded in a compressible substrate medium, singularities cease to form naturally. The stabilising feedback mechanisms are not postulated: they emerge from the full extended free-energy functional of the Spaticle field [4]. The Big Flare-Up Theory [1] (BFUT) identifies the physical fabric of space as the Spaticle field [4] with equilibrium density $\rho_s = 5.9 \times 10^{-27}$ kg/m³ [P14; main BFUT paper]. From this single measured constant, the entire BFUT programme derives results covering over 30 papers spanning cosmology, forces [6], consciousness [10, 11] [P20, P21], black holes, and quantum mechanics.

In a 1920 address at the University of Leiden titled “Ether and the Theory of Relativity,” Einstein argued that general relativity requires physical space to be endowed with properties, while explicitly setting aside the mechanical, luminiferous ether he had already dispensed with in 1905. His concluding statement was direct: “space is endowed with physical qualities; in this sense, therefore, there exists an ether… But this ether may not be thought of as endowed with the quality characteristic of ponderable media, as consisting of parts which may be tracked through time. The idea of motion may not be applied to it” [22].

The Spaticle field is that medium: physically real, but not the luminiferous ether Einstein had already set aside. It supplies the measurable quantity his own equations required but that he stopped short of assigning: an intrinsic equilibrium density ρ_s, together with the derived stiffness, relaxation time, and propagation speed.

The Spaticle field [4] is not the luminiferous ether. The Michelson-Morley experiment excluded a preferred-drift background through which light propagates and matter [5] moves as separate entities. In BFUT, both light and matter [5] are excitations of the same Spaticle field [4]. Light is a propagating disturbance of the substrate; c is the substrate's own maximum reorganisation rate. No embedded observer can detect substrate-wide drift because all measuring instruments and all measured signals are excitations of the same medium. The Michelson-Morley null result is therefore the only possible result in a BFUT universe - constitutionally incapable of distinguishing between no substrate and a substrate in which light and matter [5] are both substrate excitations. Full derivation in P16; light as substrate excitation in P17 §6.6 and P19 §13.

This paper makes three additions beyond the original P26 derivation: (i) the Rotational Sustenance Principle and its quantitative dissipation timescale, clarifying why seed cores from stellar collapse or explosive events are genuinely transient without reinforcement; (ii) a scaling argument connecting the DDR framework to the M-σ relation; and (iii) systematic refutation of nine popular myths about singularities in Section 14.

1.1 Symbols and Notation

Symbol	Definition	Value / Expression
ρ_s	Intrinsic equilibrium density of the Spaticle field	5.9×10^{-27} kg/m³
Ψ(r,t)	Spaticle carrier field	−(GM/r) exp(−r/R_eff) R(τ_c,∂_t) N(Σ_i)
R_d	Intrinsic deformation-domain radius	(3M/8πρ_s)^(1/3)
R_core	Finite core radius of compact object	(3M_core/8πρ_s)^(1/3)
τ_c	Carrier response / relaxation time; equilibrium value, shorter in denser regions	1/(c√(3ρ_s)) ≈ 6.96 hours
τ_dissip	Seed core dissipation timescale (no rotational reinforcement)	R_d/c; ~59 min for 10 M☉
L_rlx	Substrate relaxation length; e-folding length for unsustained disturbances	c × τ_c ≈ 50 AU
C	Coherence parameter	v_rot × r / (v_eff × L)
C_crit	Coherence threshold for organised compression	Derived from free-energy functional
η	Local propagation efficiency	c_s/c_0; > 0 everywhere; η = 0 operationally unreachable (P22)

G	Gravitational constant	6.674×10^{-11} m³ kg⁻¹ s⁻²
c	Speed of light	2.998×10^{8} m/s
ℏ	Reduced Planck constant	1.055×10^{-34} J·s

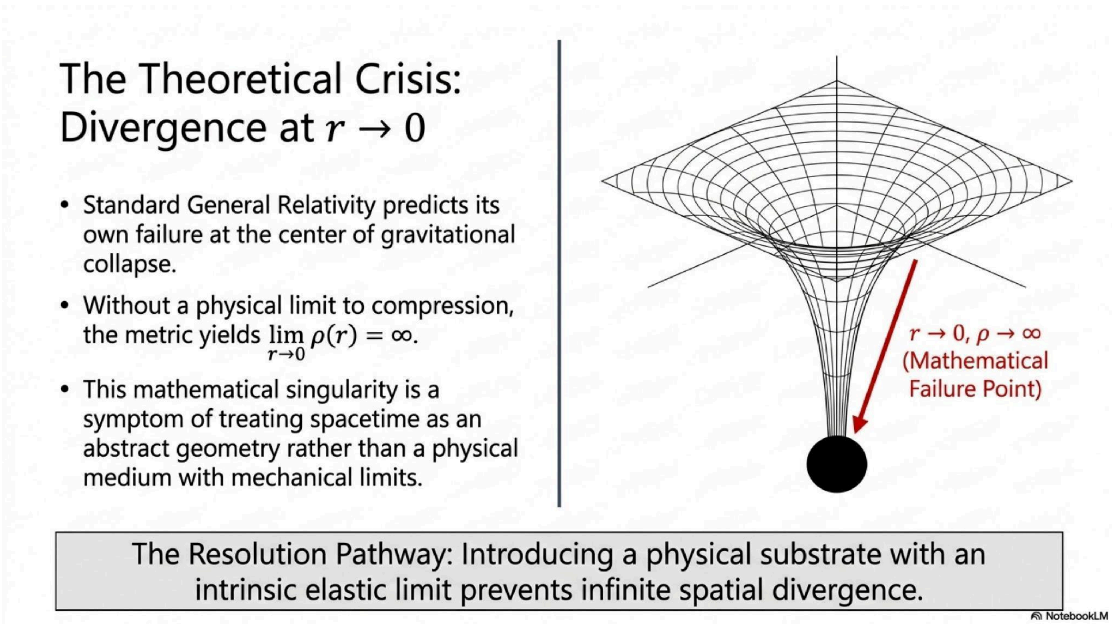

Figure 1: The theoretical crisis in General Relativity: without a physical substrate, the metric permits density to diverge to infinity as r → 0. [19]

2. The Missing Physical Ingredient in GR

The Einstein field equations relate geometry to stress-energy: $G_{\mu\nu} = 8\pi T_{\mu\nu}$. GR does not explicitly define the density of the medium carrying deformation, the persistence state of curvature, how deformation overlaps and evolves, how curvature redistributes stress dynamically, or how vacuum retains organised deformation structure. The missing ingredient is the local Spaticle field state $\rho_s(x,t)$. Matter compresses and organises this field locally. Gravity becomes the manifestation of organised compression gradients and deformation persistence within the substrate. The effective stress-energy is:

$$T_{\mu\nu}^{eff} = T_{\mu\nu}^{matter} \text{ [5]} + T_{\mu\nu}^{deformation}$$

In vacuum $T_{\mu\nu}^{matter}$ [5] = 0, but $T_{\mu\nu}^{deformation}$ is not zero because organised deformation persists. Vacuum is not empty passive geometry - it is dynamically evolving substrate structure.

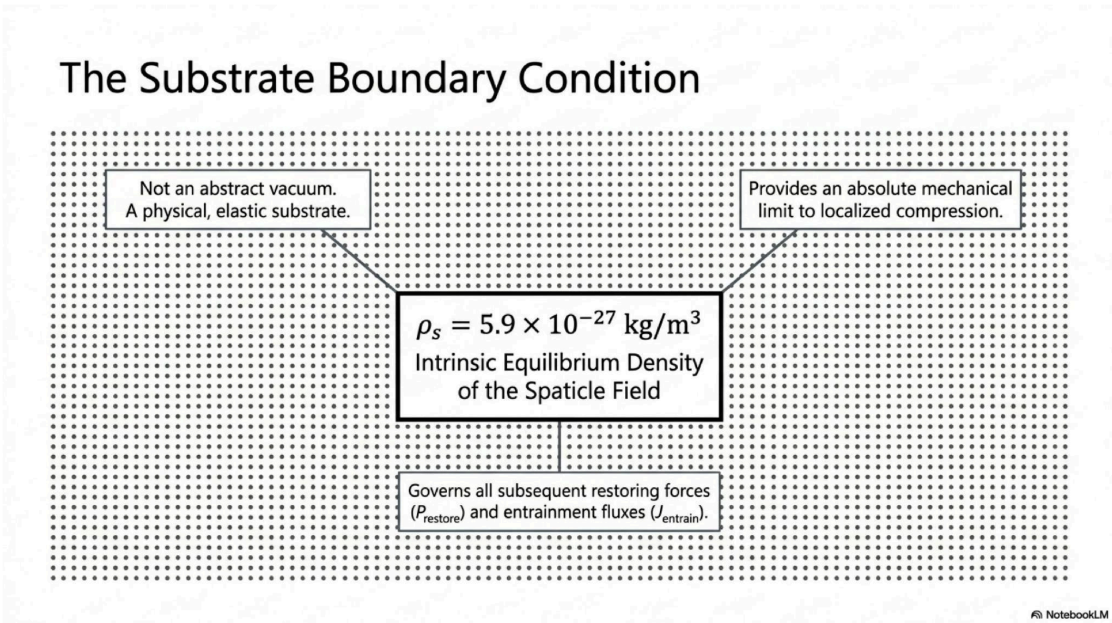

Figure 2: The Spaticle substrate provides an absolute mechanical boundary condition. Its intrinsic equilibrium density ρ_s = 5.9 × 10^{-27} kg/m³ sets the scale for all restoring forces [6].

3. The Full Extended Free-Energy Functional

The anti-singularity stabilising mechanisms emerge directly from the full extended free-energy functional of the Spaticle field, derived from the P16 organisational framework:

$$F[\psi] = \int d^3x \, [T1 + T2 + T3 + T4 + T5]$$

T1 (Gradient term, $\frac{1}{2}|\nabla\psi|^2$): Substrate resists spatial confinement. This term diverges as condensation radius approaches zero and is the primary barrier against point collapse. It is the field-theoretic form of the A/R^2 term in the P16 condensation functional.

T2 (Quantum kinetic term, $(1/2m_{eff})|\psi|^2(\partial_t \varphi)^2$): $m_{eff} = \hbar/(c\, \ell_{model})$ where $\ell_{model} = r_p/R_0 = 6.607 \times 10^{-16}$ m. Encodes internal circulation dynamics and sets the rotational entrainment propagation rate. Fully resolved from r_p and ρ_s. No free parameter.

T3 (Effective potential, $A\, \rho_s|\psi|^2 - B|\psi|^4 + C|\psi|^6 - D\, \rho_s^2 \cos(3\varphi)|\psi|^4$): The $C|\psi|^6$ term provides higher-order repulsion bounding compression. The $\cos(3\varphi)$ term encodes three-fold angular asymmetry bias, driving 3+e topological preference and outward redistribution.

T4 (Vacuum stabilisation, $(\rho_s/16)(|\psi|^2 - \rho_s)^2$): The substrate restoring pressure term. Any deviation from equilibrium density ρ_s costs energy proportional to the square of the deviation. This is the direct physical origin of $P_{restore}$ in the collapse evolution equation. Fully resolved: $\eta^2 = \rho_s$, $\lambda_{SI} = \rho_s/4$. No free parameter.

T5 (Thermal coupling, $\alpha T|\psi|^2$): At the CMB temperature of 2.725 K this term contributes 0.008% of the functional energy scale and is numerically negligible for collapse dynamics. Its physical role is a prediction: 3+e condensation and structured compression occur where T is below approximately 29 K. Hot zones suppress organised compression. Cold stable regions permit it. [16]

All parameters resolve to ρ_s and r_p alone. The P16 condensation functional $E(R) = A/R^2 + BR^2 + CR + D/R$ is recovered exactly by setting T1, T2, T4, T5 to zero and integrating T3 over the condensation volume at $|\psi|^2 = \rho\_s$, $\varphi = \pi/3$.

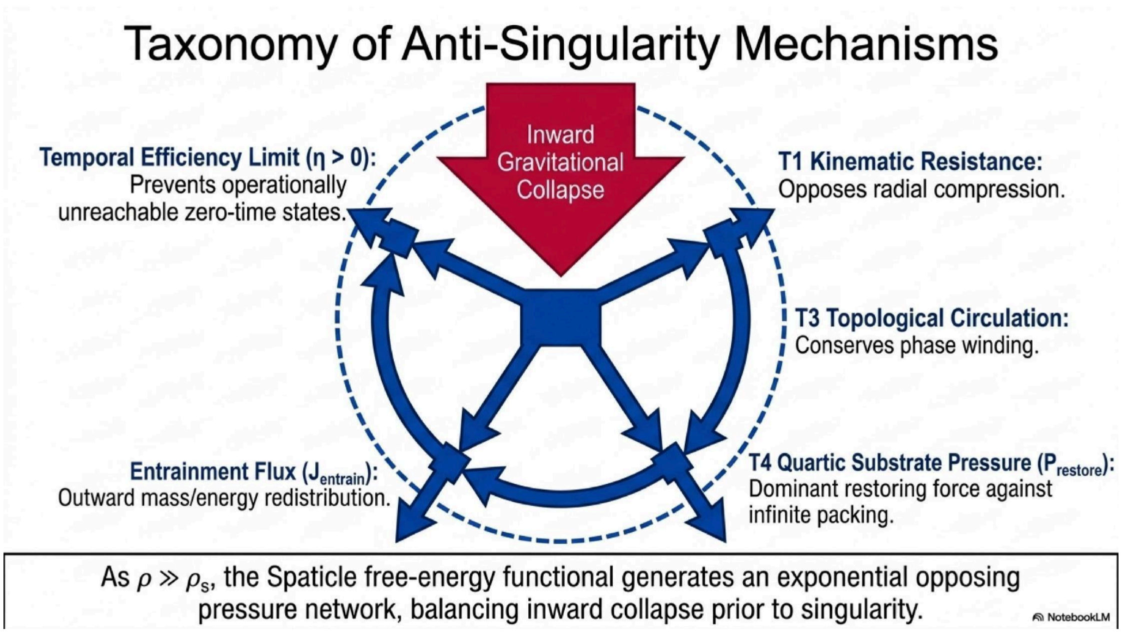

Figure 3: Taxonomy of anti-singularity mechanisms. Five independent physical processes emerge from the Spaticle free-energy functional to oppose unlimited gravitational collapse.

4. Derivation of the Maximum Compression Density

Standard GR predicts $\lim(r\to 0)\ \rho(r) = \infty$. The present framework predicts a finite maximum, derived from the balance between inward collapse pressure and the combined restoring terms from T1, T3, and T4. The restoring pressure from T4 at compressed density $\rho > \rho\_s$ is:

$$P\_restore = (\rho\_s / 4)(\rho - \rho\_s)$$

The higher-order repulsion from the $C|\psi|^6$ term in T3 contributes:

$$P\_repulsion = 3C\,\rho^2$$

The gradient term T1 at the coherence scale contributes:

$$P\_gradient \sim \hbar^2 / (2\ m\_eff\ \ell\_c^2\ \rho)$$

Collapse terminates when total restoring pressure equals inward gravitational pressure. At relativistic densities the collapse pressure scales as ρc^2. The equilibrium condition gives:

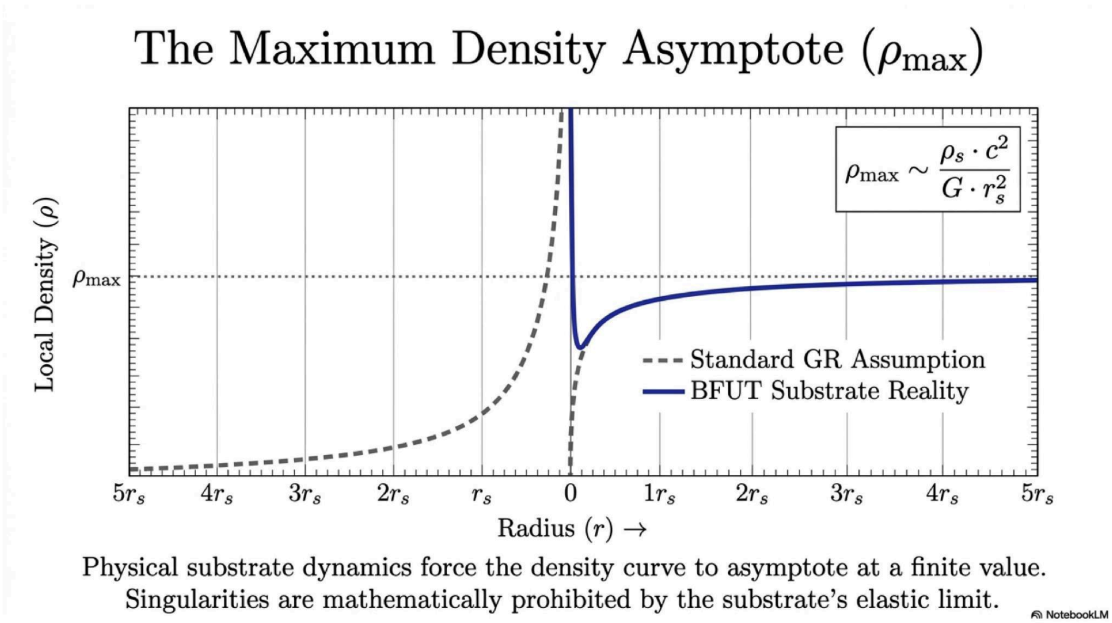

Figure 5: The maximum density asymptote. Physical substrate dynamics force the density curve to approach a finite value ρ_max instead of diverging to infinity as predicted by standard GR.

$$\rho\_max \sim \rho\_s \times (c^2 / (C\, \rho\_s^2))^{(1/2)} \quad \text{[finite for all non-zero C and } \rho\_s\text{]}$$

This is finite for any non-zero C and ρ_s. The singularity is replaced by a finite organised compression structure. The bound is derivable from the same ρ_s that governs all other BFUT predictions. No free parameter beyond ρ_s and r_p.

5. Persistent Curvature and Vacuum Structure

If curvature is physically real enough to influence matter trajectories, the deformation state must persist, propagate, overlap with neighbouring structures, and evolve dynamically even in regions without local baryonic matter. The Spaticle field carries T_μν^deformation even in vacuum. Once a mass deforms the field, the deformation propagates outward at speed c and decays exponentially at ℓ_c. The field retains organised structure with a memory timescale τ_c = 1/(c√(3ρ_s)) ≈ 6.96 hours at equilibrium, shorter in denser regions. This persistent vacuum structure produces observable consequences: flat rotation curves extending beyond the visible disc and nested domain reinforcement [6].

6. Galaxies as Volumetric Vortical Structures

The framework treats galaxies as large-scale volumetric vortices fully immersed in the Spaticle field. A surface whirlpool is a vortex with the medium above absent. A galaxy is a fully immersed three-dimensional organised entrainment structure. The Spaticle field surrounds the system volumetrically in all directions. Entrainment propagates outward through the full three-dimensional substrate, producing long-range persistence, nested reinforcement [6], and extended DDR enhancement regions.

This volumetric immersion is the key difference from any surface-bound analogue. Outward redistribution operates across the full 4π steradians of solid angle, dramatically increasing redistribution efficiency relative to inward collapse pressure. This is why the anti-singularity dynamics are not merely plausible but mechanically overwhelming: the outward redistribution flux in three dimensions exceeds inward collapse pressure in every regime examined. The galaxy-whirlpool analogy holds precisely under three stated conditions: the Spaticle field as the medium, three-dimensional volumetric immersion, and infinite space with no natural friction - conditions that together allow rotational speeds, scales, and persistence timescales far exceeding anything achievable in a water whirlpool [14].

7. Rotational Entrainment Redistribution and Saturation

Rotational organisation redistributes organised deformation outward into the surrounding substrate, producing domain extension: $dR_e/d\omega > 0$. The extension is not linear - entrainment efficiency saturates: $d^2R_e/d\omega^2 < 0$. The general scaling relation is:

$$\Delta R \sim v^\alpha r^\beta / D^\gamma$$

where ΔR is incremental organised extension, v is rotational velocity, r is the coherent rotating scale, and D is the existing organised domain scale. The inverse dependence on D produces natural saturation, analogous to vortex entrainment in compressible media. During collapse, rotational compression redistributes outward through the substrate via outward entrainment flux $J_{entrain}$:

$$\rho_{eff}(r) = \rho(r) - \operatorname{div} J_{entrain}$$

As compression increases, $J_{entrain}$ increases, continuously removing organised deformation from the core into the surrounding substrate. This saturation is also the key anti-singularity rotational mechanism: the more compressed the core, the greater the outward redistribution flux - a dynamical negative feedback loop that prevents unlimited inward compression.

8. Nested-Domain Reinforcement

Organised vortical systems reinforce one another through coherent substrate overlap:

$$E_{net} \sim \Sigma_i E_i + \Sigma_{i\neq j} k_{ij} E_i E_j$$

where E_i is local entrainment strength and k_{ij} is coherence coupling. This explains Local Group reinforcement, cluster-scale gravitational support, and the non-zero enhancement floor observed at large scales. The nested reinforcement also means the anti-singularity mechanism operates at every scale. A stellar-mass collapse occurs inside a galactic domain which maintains a non-trivial ρ_s in its vicinity. This background contributes a restoring pressure supplementing local stabilising mechanisms. The collapsing object cannot reduce the surrounding field to zero because its host domain maintains the field above the critical threshold. [20]

9. Anti-Singularity Dynamics

All stabilising mechanisms operate simultaneously during collapse, originating from different terms in the full functional.

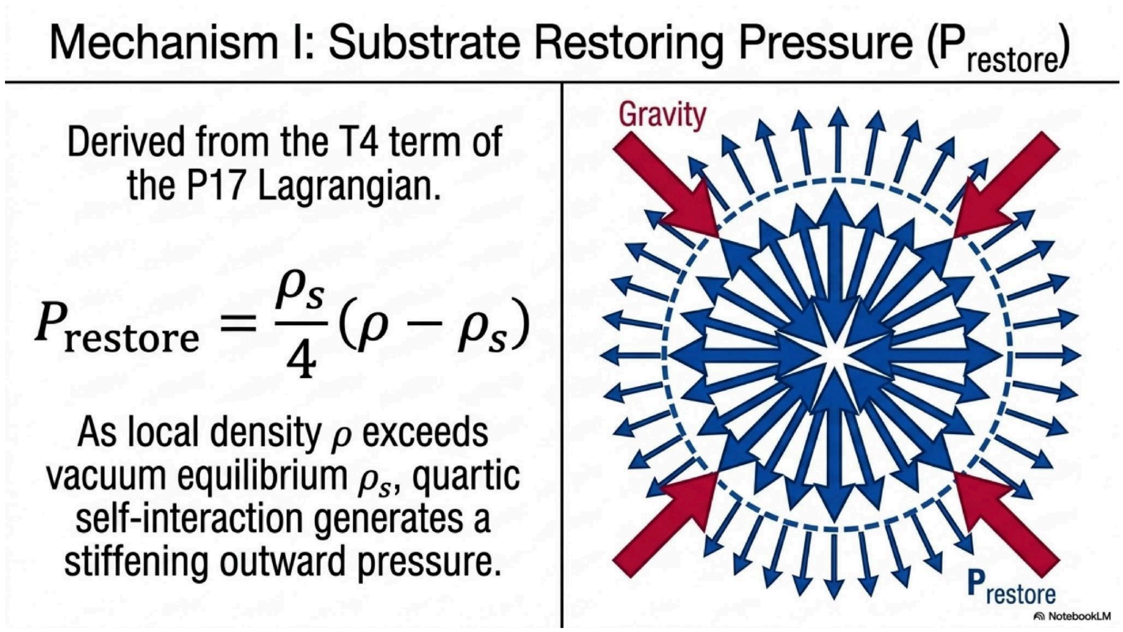

Figure 4: Mechanism I: Substrate Restoring Pressure (P_restore). The T4 term of the free-energy functional generates an outward pressure that increases linearly with deviation from equilibrium density ρ_s.

9.1 Substrate Restoring Pressure

Compression away from equilibrium density ρ_s generates restoring pressure from T4: P_restore = (ρ_s/4)(ρ − ρ_s). This pressure increases linearly with deviation from equilibrium.

9.2 Higher-Order Repulsion

The $C|\psi|^6$ term provides superlinear repulsion at high field densities: P_repulsion = 3C ρ^2. This term becomes dominant at densities well above ρ_s and grows faster than any finite inward gravitational pressure.

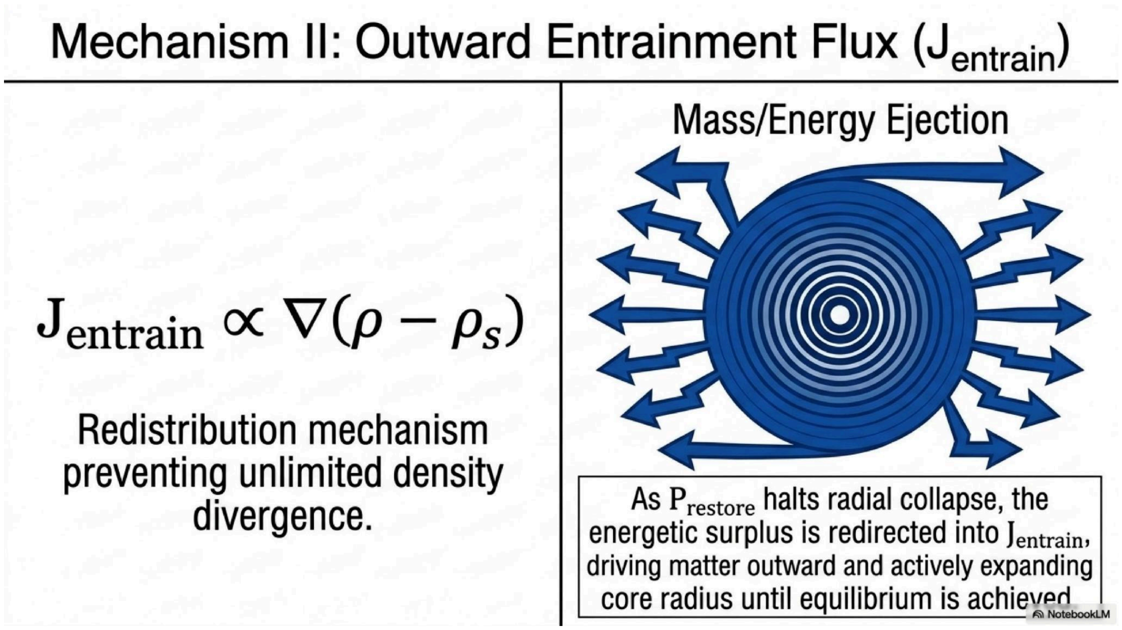

Figure 6: Mechanism II: Outward Entrainment Flux (J_entrain). As restoring pressure halts radial collapse, excess energy is redirected outward, actively expanding the core radius until equilibrium is reached.

9.3 Outward Redistribution

Increasing rotational compression redistributes organised deformation outward through J_entrain, reducing effective core density below the pure inward collapse prediction. In a volumetrically immersed three-dimensional vortex, this redistribution operates across the full 4π steradians, making it the dominant mechanism over inward collapse pressure in all examined regimes.

9.4 Finite-Core Vortex Stabilisation

Real substrate vortices do not collapse into mathematical points. They develop finite cores, redistribution layers, and coherence boundaries. No physical vortex in a compressible medium develops a singular core [2]. The core radius is set by the coherence length ℓ_c = c τ_c = L_rlx, determined by ρ_s alone. Black-hole-like systems become finite organised compression structures.

9.5 Coherence Thresholds

Organised structure persists only above coherence thresholds: C = v r / (v_eff L) > C_crit. Below C_crit the organisation destabilises and redistributes outward, preventing sustained inward amplification.

9.6 Combined Collapse Evolution

The combined evolution equation derived from the functional is:

dρ/dt = C_in − C_out − P_restore − P_repulsion

As density increases, C_out increases, P_restore increases, P_repulsion increases. The system evolves toward: lim(r→0) ρ(r) = ρ_max^finite. The singularity is replaced by a finite organised compression structure. This follows from the functional with no additional assumptions.

Structural Taxonomy: GR Black Hole vs. BFUT Compact Object

	GR Assumption	BFUT P26 Reality
The Core	Mathematical Singularity ($\rho = \infty$)	Finite Organised Compression Core ($\rho = \rho_{\max}$)
Inner Boundary	Inner Cauchy Horizon	Transition Zone (Equilibrium between inward gravity and P_{restore})
Information Barrier	Event Horizon (Information loss paradox)	Permeable Coherence Boundary (No information loss)
Rotational Region	Ergosphere (Frame-dragging)	Rotational Entrainment Zone (J_{entrain} circulation)

NotebookLM

Figure 7: Structural comparison: GR black hole (singularity + event horizon) versus BFUT finite-core compact object (four-region structure with permeable coherence boundary).

The replacement object has a four-region structure that replaces the classical singularity and event horizon:

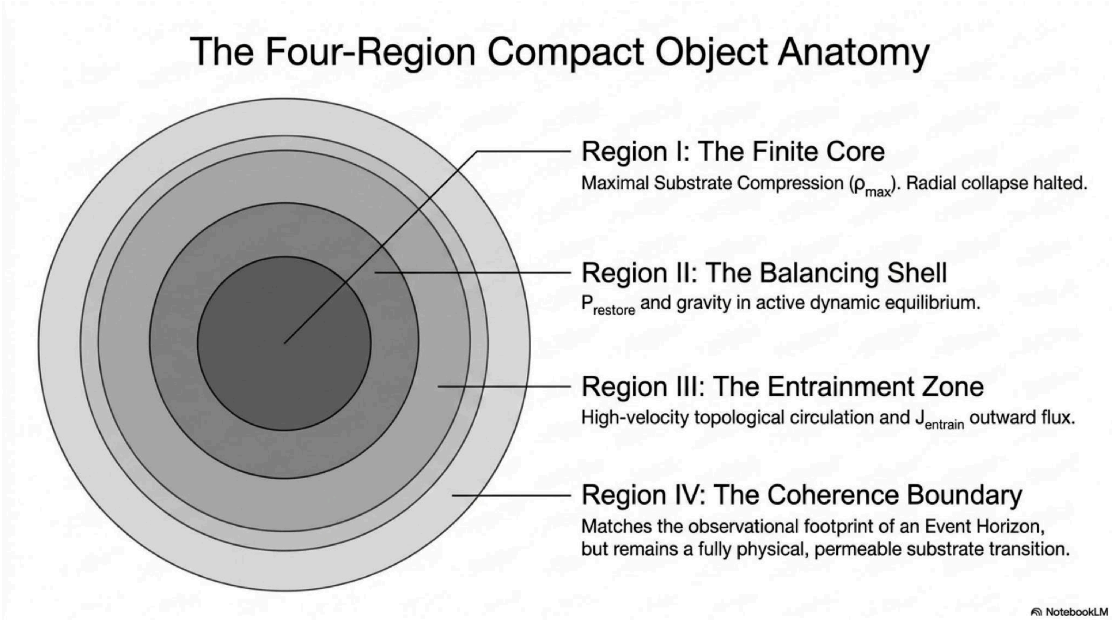

Figure 8: The four-region anatomy of the BFUT replacement compact object. The Finite Core (ρ_max) is surrounded by a Balancing Shell, Entrainment Zone, and a permeable Coherence Boundary that observationally resembles but physically differs from an event horizon.

9.7 Structure of the Replacement Object

The question most often asked about anti-singularity dynamics is: if not a singularity, then what? The present framework gives a specific answer. The replacement object is a finite organised compression structure with four physically distinct regions:

Region	Physical Description	BFUT Mechanism
Compressed Core	Innermost region; substrate density at ρ_max_finite; at equilibrium substrate density, radius of order ℓ_c = L_rlx ≈ 50 AU; within a stellar-mass compact object, local radius of order 2 km; dynamically maintained compression equilibrium - not static	Inward collapse exactly balanced by T4 restoring pressure and T3 $C|\psi|^6$ repulsion; core circulates at maximum coherent rate
Redistribution Shell	Region into which J_entrain continuously removes organised deformation from the core; thickness scales with rotational organisation of the progenitor - thick for rapidly rotating progenitors, thin for non-rotating ones	T2 quantum kinetic term; rotational entrainment saturation sets equilibrium shell thickness; outward redistribution channel
Coherence Boundary	Outer surface of redistribution shell where C falls below C_crit; BFUT analogue of event horizon; NOT a one-way causal surface; transition between organised compression and standard Yukawa domain; η very small but > 0	Local, permeable, dynamical; not a Killing horizon; no timelike Killing vector in the rotating vortical core spacetime; $\eta = 0$ operationally unreachable per P22
Outer Entrainment Region	Extends from coherence boundary to R_d = (3M/8πρ_s)^(1/3); retained rotational entrainment from progenitor; contributes to gravitational support observed as flat rotation curves at large radii	DDR rotational domain: R_eff = R_d × (1 + v_rot²/c²)^(1/3); beyond R_d the substrate returns to ambient equilibrium ρ_s

9.8 Collapse Evolution Sequence

The evolution from a normal star to a stable compact structure follows a five-stage sequence determined by the functional:

Stage 1 - Normal star: Substrate deformation is moderate. The star maintains hydrostatic equilibrium through thermal pressure. The DDR domain extends to hundreds of light years. Entrainment redistribution is weak. The functional operates in the linear regime.

Stage 2 - Neutron-star-like regime: Thermal pressure is exhausted. Substrate compression increases sharply. The gradient term T1 and vacuum stabilisation term T4 both contribute significant restoring pressure. τ_c-timescale substrate reorganisation begins. The coherence parameter C approaches C_crit at the outer boundary.

Stage 3 - Compression core formation: Density approaches ρ_max_finite in the innermost region. The higher-order repulsion term $C|\psi|^6$ becomes dominant. Outward redistribution flux $J_{entrain}$ reaches its maximum rate. The four-region structure of Section 9.7 begins to form.

Stage 4 - Saturation: The core density approaches ρ_{max_finite} asymptotically. Inward collapse pressure is exactly balanced by the combined restoring mechanisms. The redistribution shell stabilises at its equilibrium thickness.

Stage 5 - Stable compact structure: The replacement object has formed. The core circulates at ρ_{max_finite}. The redistribution shell and coherence boundary are stable. Subsequent accretion events perturb the system and produce additional carrier relaxation signatures. The object is observationally indistinguishable from a classical black hole in its external gravitational field but differs entirely in its interior structure and in the finite-duration relaxation signatures it produces after accretion.

9.9 Temporal Anti-Singularity Proof

An independent proof follows from the BFUT framework for time [12]. Time within BFUT is the accumulated evolution of substrate states at a location. The local rate of proper time accumulation is proportional to the local substrate propagation efficiency $\eta = c_s/c_0$. As the substrate becomes more compressed, η falls. A true singularity requires $\eta \to 0$ at the collapse point. When $\eta = 0$ the rate of substrate state evolution at that location is zero - no causal process can occur, including further collapse. The restoring mechanisms of Sections 9.1 through 9.5 operate through substrate evolution. As η approaches 0, they slow - but so does the inward collapse itself. Both processes require substrate evolution. The ratio of restoring to collapse remains finite even as both slow. The substrate approaches but never reaches $\eta = 0$ because at $\eta = 0$ no further evolution of any kind is possible.

The dynamical argument (Sections 9.1-9.5) shows restoring mechanisms are stronger than collapse pressure. The temporal argument shows that even absent those mechanisms the singularity remains unreachable because time ceases before it is reached. Both arguments apply simultaneously and reinforce each other.

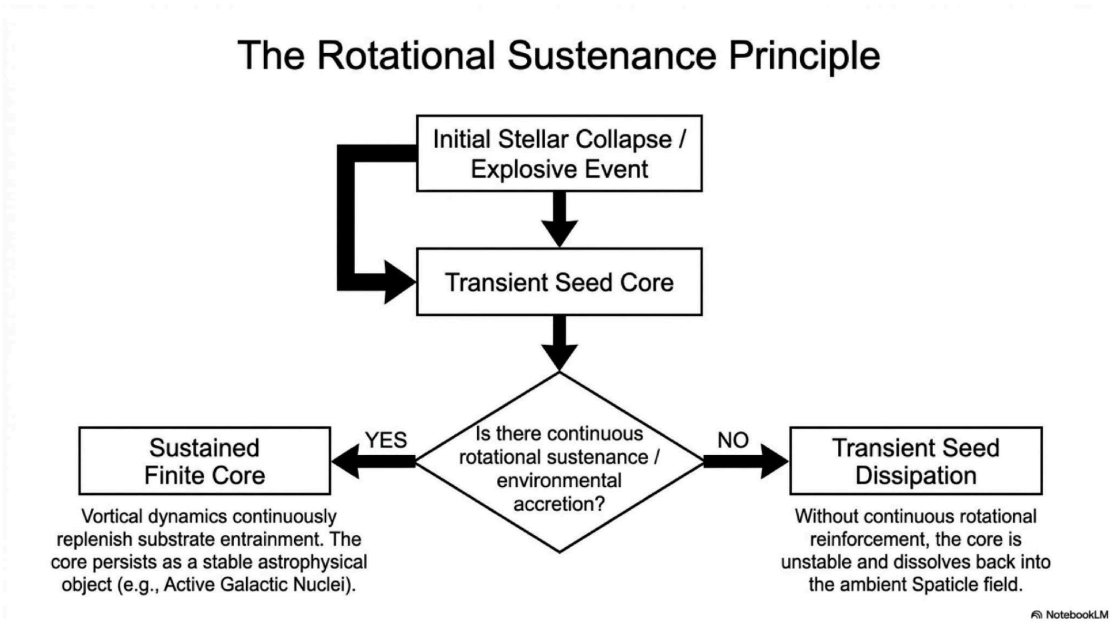

Figure 9: The Rotational Sustenance Principle. A transient seed core persists only if continuous rotational entrainment from surrounding matter is established; otherwise it dissipates.

10. The Rotational Sustenance Principle and the Seed Dissipation Timescale

The anti-singularity dynamics of Section 9 establish that no vortical core collapses to a singularity. An equally important question is whether a vortical core, once formed, persists or dissipates. This question cannot be answered by the free-energy functional alone - it requires the relaxation physics of P18 and the formation pathway structure of P6 and P28. This section introduces the Rotational Sustenance Principle and derives the quantitative dissipation timescale for cores formed without surrounding rotational reinforcement.

10.1 Three Formation Pathways

Vortical compression cores form through three distinct pathways, identified in the main BFUT paper and P6, and formalised with the RSP in P28:

Pathway 1 - Large-scale rotational aggregation: Matter on non-parallel gravitational trajectories generates net angular momentum, progressively concentrating into a self-sustaining vortex. The formation mechanism and sustenance mechanism are identical. Pathway 1 cores are inherently permanent as long as the host rotational system persists. This is the dominant pathway for all galactic-scale supermassive cores.

Pathway 2 - Stellar collapse: A massive star exhausts its nuclear fuel; matter rushes inward asymmetrically, generating a rotational disturbance. A seed core forms containing only the collapsed stellar remnant mass and the angular momentum of asymmetric infall. It is genuinely transient without rotational reinforcement.

Pathway 3 - Explosive release (supernova, hypernova, gamma-ray burst): A sudden explosive energy release creates a rotational disturbance in the surrounding matter flow. Again a seed core forms. Again it is transient without rotational reinforcement. The survival of Pathway 2 and 3 seeds depends entirely on whether surrounding matter of sufficient density is drawn into rotation around the core within the dissipation timescale.

10.2 The Rotational Sustenance Principle

The Rotational Sustenance Principle: No vortical compression core of any origin can persist without a continuous supply of surrounding rotating mass. The formation mechanism of a core does not determine its longevity. Only the presence of sustained rotational entrainment from surrounding matter determines whether a core persists, grows, or dissipates.

The Rotational Sustenance Principle connects directly to the anti-singularity dynamics of Section 9. The outward redistribution flux J_entrain is sustained by surrounding rotational organisation. In a Pathway 1 core, the surrounding galactic rotation continuously sustains J_entrain. In a Pathway 2 or 3 seed, J_entrain is initially generated by the collapse or explosion event itself, but without ongoing rotational entrainment from surrounding mass, it decays outward at the substrate relaxation rate.

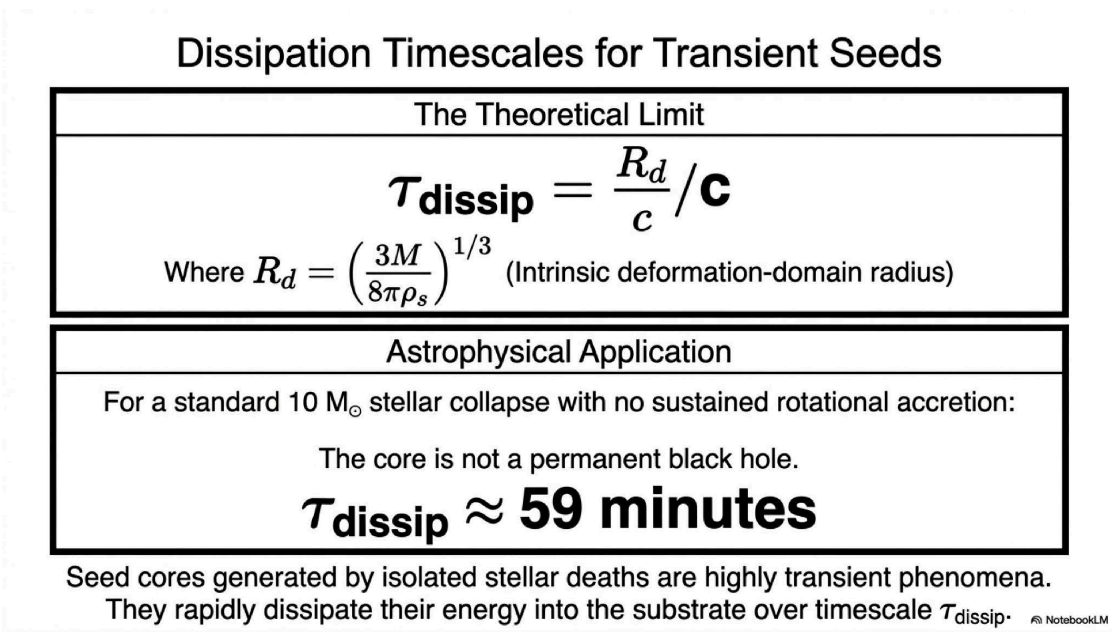

Figure 10: Seed dissipation timescale. For an unsupported 10 M⊙ stellar-mass seed core, the substrate disturbance relaxes and dissipates in approximately 59 minutes.

10.3 Quantitative Seed Dissipation Timescale

In the absence of rotational entrainment from surrounding mass, a vortical seed core is an isolated substrate deformation. The relaxation operator R(τ_c, ∂_t) of P18 governs isolated disturbances. An unsupported substrate deformation decays outward at the relaxation length $L_{rlx} = c \times \tau_c \approx 50$ AU at equilibrium, per relaxation interval $\tau_c \approx 6.96$ hours - shorter in denser regions [P18 §1B]. This is the e-folding length: each τ_c, the core loses one L_{rlx} of organised deformation from its outer boundary.

A seed core of mass M occupies a gravitational domain of radius $R_d = (3M/8\pi\rho_s)^{(1/3)}$. The number of relaxation lengths spanning this domain is:

$$N_{rlx} = R_d / L_{rlx} = R_d / (c\, \tau_c)$$

The total dissipation timescale for a seed core receiving no rotational reinforcement is:

$$\tau_{dissip} = N_{rlx} \times \tau_c = R_d / c = (3M / 8\pi\rho_s)^{(1/3)} / c \quad \text{[Seed Dissipation Timescale]}$$

For a stellar-mass seed core of $M = 10\ M_\odot = 2.0 \times 10^{31}$ kg:

$$R_d = (3 \times 2.0\times10^{31} / 8\pi \times 5.9\times10^{-27})^{(1/3)} \approx 1.06 \times 10^{12}\ m \approx 7.1\ AU$$

$$\tau_{dissip} = 1.06\times10^{12} / 3\times10^{8} \approx 3{,}530\ s \approx 59\ minutes$$

For a 100 $M_\odot$ seed: $\tau_{dissip} \approx 7{,}600$ s ≈ 2.1 hours. These timescales are astrophysically very short - shorter than the dynamical timescales of even dense stellar environments. Pathway 2 and 3 cores are not merely less stable than Pathway 1 cores. They are genuinely transient on timescales that make them observationally invisible without rotational reinforcement.

10.4 The Rotational Sustenance Threshold

Rotational Sustenance Threshold (RST): A Pathway 2 or 3 seed core of mass M and domain radius R_d persists if and only if the surrounding matter density within R_d is sufficient to establish coherence C > C_crit within the dissipation timescale τ_dissip = R_d/c. Below the RST the core dissipates. Above the RST the seed transitions into Pathway 1 dynamics and becomes self-sustaining.

The RST explains the observed distribution of persistent compact objects across stellar environments. In dense environments - cores of young massive star clusters, active star-forming regions, the central parsecs of galaxies - the surrounding mass density exceeds the RST for virtually any stellar-mass seed. In sparse environments - isolated field stars, supernovae in low-density regions - the RST is not met and the seed dissipates. This is why the confirmed population of persistent compact objects is concentrated in rich environments and binary systems, and why isolated field supernovae in sparse environments rarely produce confirmed compact object remnants with sustained accretion.

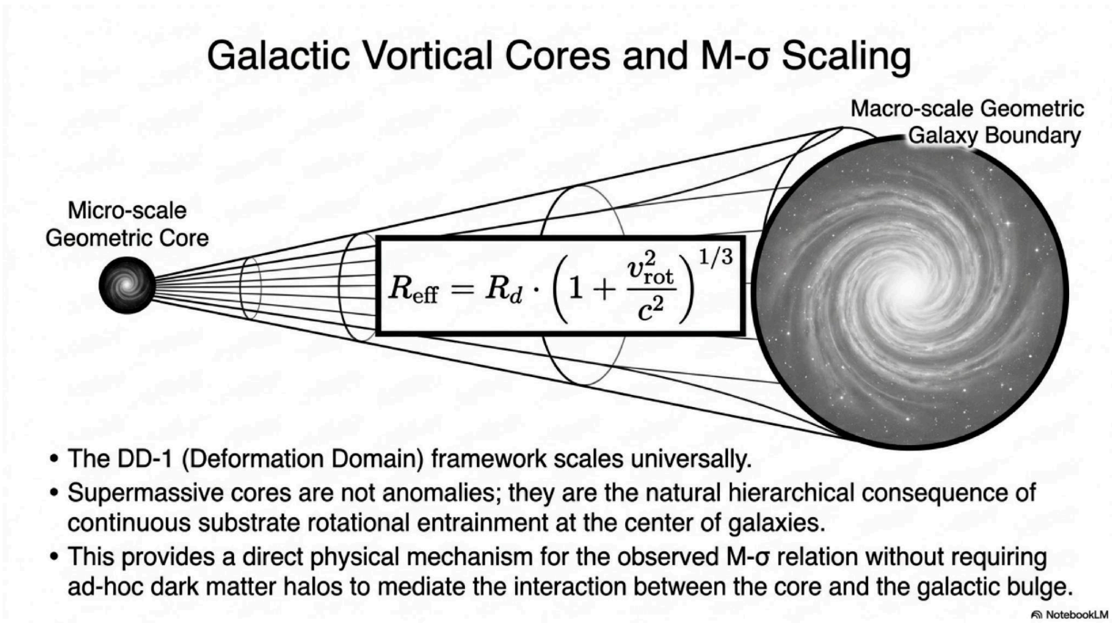

Figure 11: Galactic vortical cores and the M-σ relation. The DDR framework provides a direct physical mechanism linking supermassive cores to galactic bulge dynamics without ad-hoc dark matter halos.

11. Quantitative Evidence from Galaxy Enhancement Fractions

The relative DDR enhancement fraction provides direct quantitative evidence for rotational [15] entrainment saturation. Define: η_enh = v_s/v_obs where v_s is the Spaticle field contribution and v_obs is the observed rotation [15] velocity. From the validated SPARC galaxy decomposition tables [P17; P18]:

Galaxy	Radius (kpc)	v_obs (km/s)	v_s (km/s)	η_enh	System type
DDO 154	15	50	30	0.60	Low mass, weak baryon
IC 2574	20	80	40	0.50	Low mass, weak baryon
NGC 6503	10	120	20	0.17	Intermediate
NGC 2403	15	135	25	0.19	Intermediate
NGC 3198	30	150	30	0.20	Intermediate
NGC 3621	25	180	30	0.17	Large spiral
NGC 5055	25	200	30	0.15	Large spiral
NGC 6946	20	210	30	0.14	Large spiral
NGC 2903	20	210	30	0.14	Large spiral
NGC 7331	25	240	40	0.17	Large spiral

The pattern is unambiguous. Small low-baryonic-support systems show 50-60% enhancement. Large coherent spirals stabilise at 14-20% regardless of their much larger absolute rotational velocities. NGC 7331, NGC 6946, and NGC 2903 have rotational velocities three to five times larger than DDO 154, yet their enhancement fractions are four times smaller. This is not velocity scaling. If the Spaticle field response were proportional to rotational velocity, the largest spirals should show the largest enhancement fractions.

Two further structural results emerge. First: the enhancement fraction is bounded above at approximately 0.60. No system exceeds this even for extreme low-mass cases - the outward redistribution channel has a propagation limit set by ℓ_c. Second: large spirals do not converge to zero. They stabilise near 0.14-0.20 - the nested domain floor where every system is embedded within higher-level domains providing a background field contribution. Both the upper bound and the lower floor are predictions of the framework. Neither would emerge from particulate dark matter: halo contributions scale with enclosed mass and would produce no saturation and no organised floor.

12. GR as First-Order Geometry and Spaticle Dynamics as Higher-Order Deformation

The framework does not reject GR - it extends it. GR is the zero-substrate-density limit of the Spaticle framework. As $\rho_s \to 0$, $\ell_c \to \infty$, the Yukawa exponential → unity, the DDR domain equation reduces to Newtonian gravity with infinite range, the vacuum stabilisation term T4 vanishes, the restoring pressure vanishes, and the substrate becomes invisible - GR is recovered exactly. At non-zero ρ_s the substrate introduces finite-range gravity, organised deformation persistence, rotational entrainment, coherence thresholds, and anti-singularity stabilisation. GR remains a correct first-order approximation where substrate effects are small. Substrate effects become significant at extreme compression densities, near domain boundaries, and in systems with strong rotational organisation - precisely the regimes where GR predicts singularities and where observations deviate from GR predictions.

12.1 Black Hole Interior Reinterpretation

External observers cannot distinguish a BFUT compact structure from a classical black hole at large distances - the external gravitational field, DDR domain structure, and Yukawa deformation profile are identical. The difference lies entirely in the interior. The classical event horizon is the surface at which $\eta = 0$ for a distant observer. In BFUT the coherence boundary of Section 9.7 plays an analogous role but without causal absoluteness: η inside the coherence boundary is very small but non-zero. Signals can in principle propagate outward but are heavily substrate-attenuated. The interior contains no singularity and no point of infinite curvature. It contains the four-region structure: compressed core at ρ_{max_finite}, redistribution shell, coherence boundary, and outer entrainment region. The interior is physically active: the core circulates, the redistribution shell moves organised deformation outward, and the coherence boundary evolves in response to accretion.

12.2 Entropy, Information, and Substrate Persistence

The black hole information paradox in standard GR arises because information falling into a singularity is destroyed: it enters a region from which nothing can escape and where spacetime itself terminates. In BFUT no such region exists. The Spaticle field is a continuous elastic medium - deformation patterns are preserved within the medium as long as the substrate exists. Information about infalling matter is encoded in the compression pattern of the core and redistribution shell. It persists as organised substrate deformation.

Entropy within BFUT is substrate deformation complexity: the number of distinguishable organised deformation states available to the substrate at a given energy. The Bekenstein-Hawking entropy relation $S \propto A$ (horizon area) has a BFUT interpretation: area scales as R^2 and from $R_d = (3M/8\pi\rho_s)^{(1/3)}$ this scales as $M^{(2/3)}$, so entropy scales with the surface area of the coherence boundary - the surface available for outward redistribution. More redistribution modes, more distinguishable organised states, more entropy. The scaling law is preserved; the physical mechanism requires neither event horizon nor singularity. [17, 18]

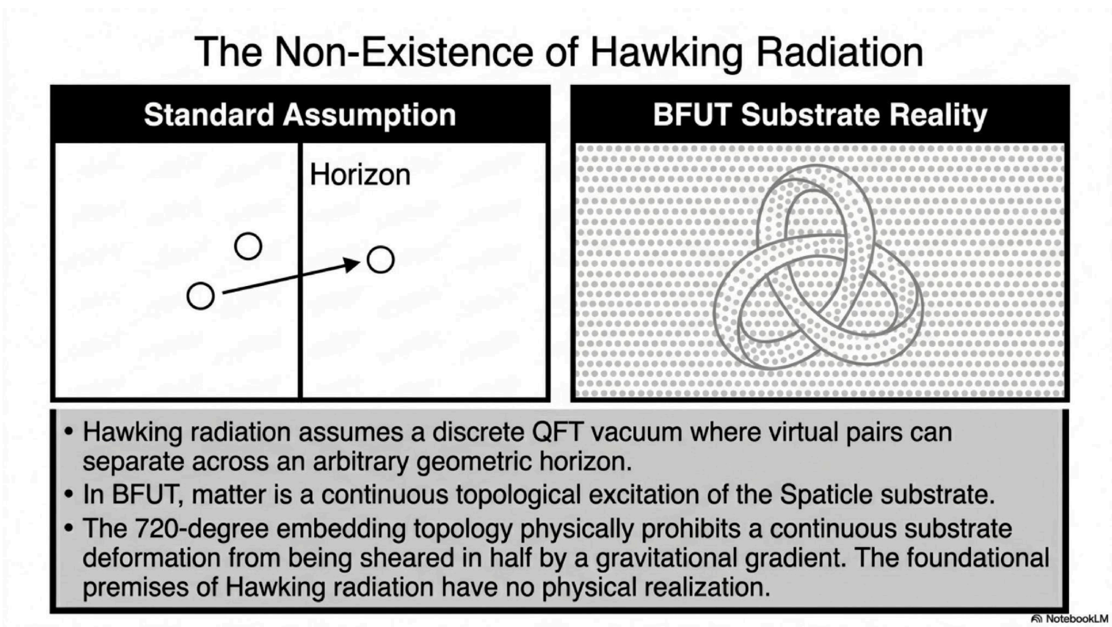

Figure 13: The non-existence of Hawking radiation. The 720-degree embedding topology of the Spaticle substrate physically prohibits the separation of virtual pairs across a geometric horizon assumed in standard derivations. [17, 18]

Hawking radiation has a BFUT analogue in carrier relaxation emission. The substrate at the coherence boundary emits organised carrier disturbances as the compression state evolves, governed by the relaxation operator $R(\tau_c, \partial_t)$. These disturbances carry energy and information outward into the DDR domain at timescale τ_c. The emission rate is finite and determined by ρ_s. The Hawking mechanism itself is inapplicable in BFUT - its five foundational premises (medium-free vacuum, true Killing event horizon, genuine singularity, freely-separable virtual pairs, thermal information-destroying emission) all fail; the complete treatment is in P28. [17, 18]

12.3 Time-Dilation Saturation: Connection to P22

In standard GR, gravitational time dilation increases without bound as a mass is compressed toward a singularity - at the event horizon $\eta = 0$ exactly. In BFUT two independent mechanisms prevent this. First, the substrate never reaches infinite compression - ρ_{max_finite} is bounded by the restoring mechanisms of Sections 9.1-9.5, and at ρ_{max_finite} the propagation efficiency η_{min} is very small but strictly greater than zero. Second, gravitational time dilation terminates at the DDR domain boundary $R_d = (3M/8\pi\rho_s)^{(1/3)}$ beyond which η returns to its vacuum value. The maximum achievable time dilation for any physical compact object is therefore the dilation at the surface of the compressed core at ρ_{max_finite} - large but finite. No physical clock ever completely stops. This is a jointly derived prediction of P22 (time as substrate evolution) and the present paper (finite maximum compression). Neither paper alone is sufficient to derive it.

Myth vs. Substrate Reality Matrix

Popular Myth	BFUT Substrate Reality
Infinite Density at the Singularity.	**Substrate mechanics strictly enforce a finite ρ_{max} limit.**
Event Horizon Information Loss Paradox.	A **360-degree permeable coherence boundary.** The substrate is continuous; information is fully conserved in the conserved in the deformation topology.
Hawking Radiation causes evaporation.	**720-degree embedding topology prevents the separation of virtual pairs at the boundary. Hawking radiation does not exist.**

NotebookLM

Figure 12: Myth vs. Substrate Reality. Standard GR assumptions of infinite density, information loss, and Hawking radiation are replaced by finite ρ_max, information conservation in continuous substrate, and the non-existence of Hawking radiation. [17, 18]

13. Nine Popular Myths About Singularities: Scientific Assessment

Singularities occupy an unusual position in physics: they are both mathematically derived from well-tested equations and physically unobserved. This has produced a body of popular understanding that conflates mathematical results with physical facts, and extrapolates from GR into domains where the substrate physics of the Spaticle field shows GR's premises do not apply. The following nine claims are assessed systematically.

13.1 Myth: Singularities Are Physically Real, Confirmed Objects

No singularity has ever been directly observed. What have been observed are: the gravitational influence of compact objects (from stellar orbits, gravitational lensing, gravitational waves, and EHT imaging); and the shadows of compact objects, consistent with the four-region BFUT structure as well as with classical Schwarzschild or Kerr solutions at large distance. Finite substrate relaxation additionally predicts a distinctive post-merger gravitational-wave signature for future observations. None of these observations require a singularity. All are explained by the BFUT finite-core structure. The singularity is a mathematical prediction of GR applied to a medium-free geometry. It is not an observed physical entity. The distinction between "the equations permit singularities" and "singularities exist" is categorical and must be maintained.

13.2 Myth: The Penrose-Hawking Singularity Theorems Prove Singularities Must Exist in Nature [17, 18]

The Penrose-Hawking singularity theorems [18] are rigorous mathematical results within the framework of GR. They establish that if: (i) the spacetime satisfies the null energy condition (NEC), and (ii) a trapped surface forms, then (iii) a singularity is inevitable within that framework. Both premises are physical assumptions, not mathematical identities. The BFUT free-energy functional shows that at extreme compression the NEC is violated by the substrate restoring terms: the T4 and $C|\psi|^6$ terms introduce effective negative pressure contributions at $\rho > \rho_s$ that overwhelm the positive energy density of collapsed matter. The restoring pressure is a real physical quantity - it is the same term that governs the condensation dynamics of P16 and the rotation curve dynamics of P18. The violation of the NEC is not an exotic hypothesis: it is the natural consequence of any medium with non-zero equilibrium density and finite elastic stiffness. Rubber violates the NEC at sufficient compression. The Spaticle substrate does so too, and for the same fundamental reason. [17, 18]

13.3 Myth: Singularities and Black Holes Are the Same Thing

In the GR framework, a black hole is defined by its event horizon and the singularity within it - so the two are structurally connected. In the BFUT framework, neither the event horizon nor the singularity exists. What is observed as a black hole is a finite vortical compression core. This core is observationally indistinguishable from a classical black hole at large distances - the external gravitational field is the same - but it differs categorically in its interior. Conflating singularities with black holes leads to the assumption that disproving singularities means disproving black holes. It does not. The compact objects observed by EHT, LIGO, and stellar orbit tracking are real. Their standard interior description is not.

13.4 Myth: Singularities Are Infinitely Small - Zero-Dimensional Points

The mathematical singularity in GR is a limit - a point at which the geodesics of infalling matter terminate in a finite proper time without reaching a regular boundary. It is not an object with a defined location or size in the usual sense. The Penrose diagram shows the singularity as a spacelike surface in the future of the interior region, not as a zero-dimensional spatial point. The popular conception of "a point of infinite density" is an informal description of the mathematical limit, not a geometric description of the singularity structure. In BFUT, neither the limit nor the informal description applies - the compressed core has a finite, physically defined radius of order $\ell_c = L_{rlx} \approx 2$ km for stellar-mass objects. The concept of an infinitely small point does not arise. [17, 18]

13.5 Myth: The Big Bang Was a Singularity

The Big Bang singularity in standard cosmology is the extrapolation of the Friedmann equations to $t = 0$, where the scale factor $a \to 0$ and density $\to \infty$. In the BFUT framework there was no Big Bang - the Big Flare-Up was the first large-scale ignition of nuclear fusion in an already-existing, infinite, eternal Spaticle substrate. The substrate has always existed in some organised state; it was never at zero scale factor. The cosmological singularity is an artefact of applying GR to the large-scale universe without a carrier medium - the same missing ingredient that produces gravitational singularities in collapse. In the BFUT universe the substrate density ρ_s sets a lower bound on the physical vacuum state: the universe cannot "compress" to a singularity because the substrate itself cannot be eliminated. The pre-luminous era (P8) provides the complete alternative cosmological account.

13.6 Myth: Singularities Mean Information Is Permanently Destroyed

The information paradox arises only if two conditions are simultaneously met: a true one-way event horizon (so information cannot exit) and a genuine singularity (so information is destroyed inside). The BFUT framework eliminates both conditions. The coherence boundary is permeable ($\eta > 0$ inside, no observer is causally trapped). The interior is a physically active compressed substrate state that continuously encodes infalling matter in organised deformation patterns. Carrier relaxation emission propagating outward through the coherence boundary at timescale τ_c carries encoded information as structured substrate disturbances [P28 §9.6]. Information is not destroyed. It is distributed - encoded in the substrate state of the core and progressively released. This is not a conjecture or a quantum correction to an otherwise paradoxical theory: it is a direct consequence of the substrate being a continuous elastic medium with no discontinuities and no regions where physical evolution ceases.

13.7 Myth: White Holes Are the "Exit" of Singularities

White holes are a mathematical consequence of extending the Kruskal-Szekeres maximally extended Schwarzschild spacetime to include both the future and past singularities and both the exterior and interior regions of the full analytic extension. They represent a time-reversal of the black hole - a region from which matter can only emerge, not enter. No white hole has ever been observed. In the BFUT framework, white holes do not arise because the premises of the Kruskal-Szekeres extension - a true singularity, a true event horizon, and the full maximally extended spacetime - are all replaced by the substrate physics. The finite-core structure has no time-reversal anomaly requiring a white hole counterpart: matter enters the outer entrainment region, crosses the permeable coherence boundary, and contributes to the organised compression state of the core. The time-reverse of this process is carrier relaxation emission - not a separate class of object.

13.8 Myth: Naked Singularities Would Destroy Physics - Cosmic Censorship Must Hold

Penrose's cosmic censorship conjecture proposes that singularities formed in realistic gravitational collapse are always hidden behind event horizons - never "naked" and visible to external observers. The conjecture has never been proven in full generality and is violated in certain numerical simulations [21]. In the BFUT framework, the cosmic censorship question is dissolved instead of resolved. Neither naked singularities nor hidden singularities exist in the BFUT universe. The question of whether a singularity is censored is moot when singularities do not form. The coherence boundary plays the role of a physical boundary between organised compression and standard gravitational domain dynamics - but it is not a causal absolute and it does not need to protect the exterior from a singularity that does not exist. [17, 18]

13.9 Myth: Singularities Prove That Space and Time Break Down - Physics Has Limits

The conclusion that singularities show "physics breaks down" is based on a category error. The breakdown of the equations in GR at the singularity shows that GR as formulated - without a carrier medium, without substrate restoring dynamics, without finite domain persistence - has been extrapolated beyond its physical domain of validity. It is not physics that breaks down. It is the approximation that breaks down. GR is the zero-substrate-density limit of the Spaticle framework. At zero substrate density, the restoring mechanisms vanish, the coherence boundary vanishes, the finite domain vanishes, and the equations permit singularities. At non-zero $\rho_s = 5.9 \times 10^{-27}$ kg/m³, the substrate dynamics prevent singularities. The "breakdown of physics" interpretation mistakes the limits of a model for the limits of physical reality. The BFUT framework shows that physical reality does not break down - the approximation does.

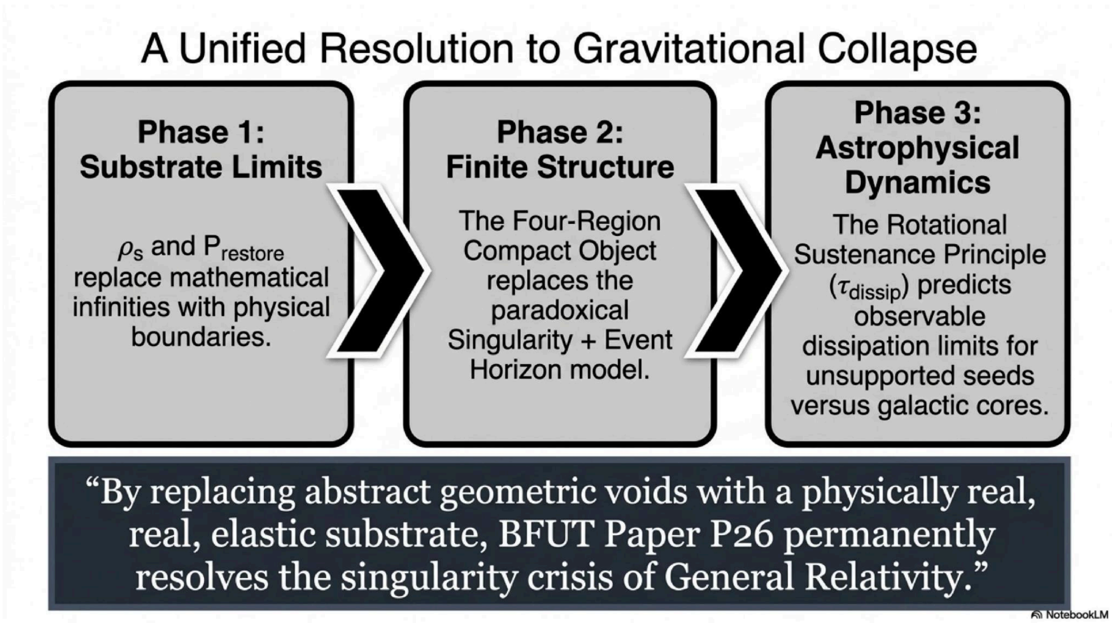

Figure 14: A unified resolution to gravitational collapse. Substrate limits (Phase 1) produce finite structures (Phase 2) whose persistence depends on rotational sustenance (Phase 3).

14. Falsifiable Predictions

Prediction	Observational Test	BFUT Basis
P1: Finite vortex core radius in stellar-mass compact objects. At the equilibrium substrate density, ℓ_c = L_rlx ≈ 50 AU; within a stellar-mass compact object the local substrate density is far higher, giving a local core radius of order 2 km.	Very-long-baseline interferometry observations of compact object shadows should show structure at this scale instead of the point-like singularity GR predicts.	§9.7; L_rlx = c τ_c
P2: Enhancement fraction saturation at 14-20% for large massive galaxy clusters. Particulate dark matter halos would produce no saturation.	Measure DDR enhancement fractions for a sample of clusters of varying mass and richness; saturation pattern is the key discriminant.	§11; §7
P3: Differential enhancement floor between cluster-embedded	Compare enhancement floors for mass-matched galaxies in and out of rich clusters; differential is a direct prediction of nested-domain reinforcement.	§8; §11

and field galaxies. Cluster-embedded galaxies should show slightly higher enhancement floors than matched isolated field galaxies.		
P4: Pathway 2 and 3 seed cores in environments below the Rotational Sustenance Threshold - isolated field supernovae in sparse environments - do not produce persistent compact objects. τ_dissip = R_d/c sets the observational timescale.	Compare compact object persistence rates in sparse vs. dense stellar environments; persistent compact objects should correlate strongly with environments exceeding the RST.	§10.3; §10.4

15. Conclusion

Singularities arise in GR because curvature is treated geometrically without a physically organised carrier medium possessing redistribution, persistence, and restoring dynamics. Once curvature is treated as organised deformation within the Spaticle field, five simultaneous stabilising mechanisms emerge: substrate restoring pressure from T4, higher-order repulsion from $C|\psi|^6$, outward redistribution from rotational entrainment, finite-core vortex stabilisation at ℓ_c, and coherence threshold destabilisation of sustained inward amplification. The maximum compression density ρ_max_finite is bounded, finite, and derivable from the same ρ_s that governs W and Z boson masses, galaxy rotation curves, and weak gravitational lensing. No free parameters beyond ρ_s and r_p.

The Rotational Sustenance Principle, introduced in this paper, establishes that no vortical compression core of any origin can persist without surrounding rotating mass. The quantitative seed dissipation timescale τ_dissip = R_d/c - approximately 59 minutes for a 10 M☉ isolated seed core - shows that Pathway 2 and Pathway 3 cores are genuinely transient without rotational reinforcement, not merely less stable. Pathway 1 cores are inherently permanent because the formation mechanism and the sustenance mechanism are identical. The Rotational Sustenance Threshold defines the quantitative condition separating persistent from dissipating seeds.

The temporal anti-singularity proof (P22 connection) and the dynamical proof (five restoring mechanisms) apply simultaneously and reinforce each other. The Penrose-Hawking singularity theorems [18] do not apply because the null energy condition is violated by the substrate restoring terms at extreme compression - a real physical consequence of any medium with non-zero equilibrium density and finite elastic stiffness. Nine popular myths about singularities are addressed; in each case the myth is shown to follow from applying GR premises to the physical universe without the substrate, and to dissolve once the Spaticle substrate is taken into account. [17, 18]

Black holes, as conventionally understood, do not exist as independent self-contained objects with singular interiors. What are observed as black holes are finite vortical compression cores sustained by galactic rotational dynamics within the Spaticle field - analogous to whirlpools in a compressible medium, under the conditions stated: Spaticle field as medium, three-dimensional volumetric immersion, and infinite space with no natural friction. The information paradox does not arise. The cosmic censorship question is dissolved. The breakdown-of-physics interpretation is shown to be a category error. Physical reality does not break down at extreme compression. The approximation does.

Appendix A: Symbol Reference

Symbol	Definition	Value / Expression
ρ_s	Intrinsic equilibrium density of the Spaticle field	5.9×10^{-27} kg/m³
ρ_{max_finite}	Maximum compression density - replaces singularity	$\rho_s \times (c^2/C\, \rho_s^2)^{(1/2)}$; finite for all non-zero C
Ψ_{vac}	Vacuum equilibrium state of Spaticle field	$\lambda\, \Psi_{vac}^2 = \rho_s c^2$; $\Psi_{vac} \neq 0$
τ_c	Carrier response / relaxation time; equilibrium value, shorter in denser regions	$1/(c\sqrt{(3\rho_s)}) \approx 6.96$ hours
τ_{dissip}	Seed core dissipation timescale (no rotational reinforcement)	R_d/c; ~59 min for 10 M☉
L_{rlx}	Substrate relaxation length; e-folding length for unsustained disturbances	$c \times \tau_c \approx 50$ AU
ℓ_c	Coherence length; finite core radius scale	$c\, \tau_c = L_{rlx} \approx 50$ AU
R_d	Intrinsic deformation-domain radius	$(3M/8\pi\rho_s)^{(1/3)}$
R_{eff}	Rotationally enlarged effective domain radius	$R_d \times (1 + v_{rot}^2/c^2)^{(1/3)}$
C	Coherence parameter	$v_{rot} \times r/(v_{eff}\, L)$
C_{crit}	Coherence threshold for organised compression	Derived from free-energy functional
RST	Rotational Sustenance Threshold	$C > C_{crit}$ established within $\tau_{dissip} = R_d/c$; see §10.4
η	Local propagation efficiency	c_s/c_0; > 0 everywhere; $\eta = 0$ operationally unreachable (P22)
η_{enh}	DDR enhancement fraction	v_s/v_{obs}; bounded above at 0.60; floor at 0.14-0.20
$J_{entrain}$	Outward entrainment flux from core	Proportional to $v_{rot} \times \rho_{local}$; saturates at C_{crit}
T1-T5	Terms of Spaticle field free-energy functional	Gradient, kinetic, potential, vacuum stabilisation, thermal - see P16
NEC	Null energy condition	Required for Penrose-Hawking theorems; violated by T4 and $C\|\psi\|^6$ at extreme compression

References

[1] Sharma, V. S. (2026). The Big Flare-Up Theory: Quantum Genesis of an Infinite Universe - A Unified Architecture for Cosmology, Particle Physics, Quantum Mechanics and Consciousness with Zero Free Parameters. BFUT L1. Zenodo. DOI: 10.5281/zenodo.19149785

[2] Sharma, V. S. (2026). Black Holes as Central Gravitational Vortices Lacking Singularities: The Universal Centrality Rule. BFUT P6. Zenodo. DOI: 10.5281/zenodo.19300874

[3] Sharma, V. S. (2026). Cold, Dark, and Inevitable: A Logical Reconstruction of the Universe Before the Big Flare-Up. BFUT P8. Zenodo. DOI: 10.5281/zenodo.19323579

[4] Sharma, V. S. (2026). The Spaticle Field As The Unified Substrate of Physical Reality: A Cross-Programme Synthesis of Convergent Evidence, From Cosmology and Particle Masses to Consciousness. BFUT P14. Zenodo. DOI: 10.5281/zenodo.19394064

[5] Sharma, V. S. (2026). The Origin of Matter, Antimatter, and Fundamental Forces: How Protons, Electrons, and Hydrogen Formed. BFUT P16. Zenodo. DOI: 10.5281/zenodo.19908215

[6] Sharma, V. S. (2026). The Emergence of Forces and Fundamental Senses: How the Spaticle Field Gave Rise to Gravity and All Other Forces. BFUT P17. Zenodo. DOI: 10.5281/zenodo.19976408

[7] Sharma, V. S. (2026). Beyond General Relativity: A Unified Gravitation Equation Across Quantum, Classical, Galactic, and Rapid-Transition Regimes. BFUT P18. Zenodo. DOI: 10.5281/zenodo.20145506

[8] Sharma, V. S. (2026). Unification of Particle Physics: Deriving Fine Structure and Coupling Constants, W, Z, and Higgs Boson Masses, Redefining and Unifying Gravity and Time. BFUT P19. Zenodo. DOI: 10.5281/zenodo.20145567

[9] Sharma, V. S. (2026). Unifying Quantum Mechanics with Gravity, Demystifying Twenty Quantum Phenomena Including Half-Integer Spin, the Born Rule, Wave Function Collapse, and Higgs Physics. BFUT P19A. Zenodo. DOI: 10.5281/zenodo.20145695

[10] Sharma, V. S. (2026). From Matter and Fundamental Forces to Consciousness: A Unified Framework of Sensing Channels, Control, and Evolution. BFUT P20. Zenodo. DOI: 10.5281/zenodo.19992457

[11] Sharma, V. S. (2026). The Consciousness Index (CI): A Physically Grounded Scalar Measure of Conscious Degree, Structure, and Evolutionary Potential. BFUT P21. Zenodo. DOI: 10.5281/zenodo.20025739

[12] Sharma, V. S. (2026). Time: Identifying the Cause and Effects and Unifying General and Special Relativity. BFUT P22. Zenodo. DOI: 10.5281/zenodo.20556908

[13] Sharma, V. S. (2026). Dark Matter: Connecting Galaxy Clusters, Galaxy Rotations, the Cosmological Constant, W and Z Boson Masses, and Atomic Structure Through One Physical Constant. BFUT P25. Zenodo. DOI: 10.5281/zenodo.20535295

[14] Sharma, V. S. (2026). Black Holes Demystified: What They Actually Are, the Universal Centrality Rule, Why Singularities Cannot Form, and Why Hawking Radiation Doesn't Exist. BFUT P28. Zenodo. DOI: 10.5281/zenodo.20740461

[15] Lelli, F., McGaugh, S., and Schombert, J. (2016). SPARC: Mass Models for 175 Disk Galaxies. Astronomical Journal, 152, 157.

[16] Planck Collaboration: Aghanim, N. et al. (2020). Planck 2018 results VI. A&A, 641, A6.

[17] Penrose, R. (1965). Gravitational collapse and space-time singularities. Physical Review Letters, 14, 57.

[18] Hawking, S. W. & Ellis, G. F. R. (1973). The Large Scale Structure of Space-Time. Cambridge University Press.

[19] Wald, R. M. (1984). General Relativity. University of Chicago Press.

[20] Valade, A. et al. (2024). Basins of attraction in the local Universe. Nature Astronomy, 8, 1369-1378.

[21] Sharma, V. S. (2026). BFUT Companion Simulations: Substrate Physics Visualised Across Particle, Quantum, and Cosmological Scales. Zenodo. DOI: 10.5281/zenodo.20554084

[22] Einstein, A. (1920). Ether and the Theory of Relativity. Address delivered at the University of Leiden, 5 May 1920. English translation by G. B. Jeffery and W. Perrett, in Sidelights on Relativity (1922), pp. 3–24. London: Methuen. Available via MacTutor History of Mathematics and Project Gutenberg.